Energy Engineering

Tech Science Press

DOI: 10.32604/ee.2022.020011

ARTICLE

Distributionally Robust Optimal Dispatch of Virtual Power Plant Based on Moment of Renewable Energy Resource

Wenlu Ji, Yong Wang*, Xing Deng, Ming Zhang and Ting Ye

Nanjing Power Supply Company of State Grid Jiangsu Electric Power Co., Ltd., Nanjing, 210019, China

*Corresponding Author: Yong Wang. Email: wangyongnjj@126.com

Received: 29 October 2021 Accepted: 12 January 2022

ABSTRACT

Virtual power plants can effectively integrate different types of distributed energy resources, which have become a new operation mode with substantial advantages such as high flexibility, adaptability, and economy. This paper proposes a distributionally robust optimal dispatch approach for virtual power plants to determine an optimal day-ahead dispatch under uncertainties of renewable energy sources. The proposed distributionally robust approach characterizes probability distributions of renewable power output by moments. In this regard, the faults of stochastic optimization and traditional robust optimization can be overcome. Firstly, a second-order cone-based ambiguity set that incorporates the first and second moments of renewable power output is constructed, and a day-ahead two-stage distributionally robust optimization model is proposed for virtual power plants participating in day-ahead electricity markets. Then, an effective solution method based on the affine policy and second-order cone duality theory is employed to reformulate the proposed model into a deterministic mixed-integer second-order cone programming problem, which improves the computational efficiency of the model. Finally, the numerical results demonstrate that the proposed method achieves a better balance between robustness and economy. They also validate that the dispatch strategy of virtual power plants can be adjusted to reduce costs according to the moment information of renewable power output.

KEYWORDS

Virtual power plant; optimal dispatch; uncertainty; distributionally robust optimization; affine policy

1 Introduction

Renewable energy sources, including wind farms and photovoltaic arrays, have experienced explosive growth during the past few years. Besides, the transformation from centralized energy resources to distributed energy resources has become an evitable trend, owing to the advantages of distributed energy resources such as reliability, economy, flexibility, and environment friendly. However, serious problems also exist for distributed energy resources, such as small capacity, geographical dispersion, and stochastic power output, which present great challenges to the effective control of electric power systems. These risks can be mitigated by an effective technology called virtual power plants. Virtual power plants are aggregate portfolios to manage different types of distributed energy resources, such as conventional generation units, renewable energy sources, storages, and load demands, through

advanced communication, measurement, and control techniques [1,2]. Such aggregation enables distributed energy resources with complementary advantages to improve the overall stability and realize the scale merit. The resulting aggregation also enables distributed energy sources with adequate dimensions to participate in electricity markets as an integrated entity, which provides the opportunity for the owners of distributed energy resources to seek more profits [3]. In this context, virtual power plants have been developed rapidly in recent years, making the utilization of distributed energy resources more flexible, adaptive, and profitable [4].

The randomness and uncertainty of renewable power output in virtual power plants have posed severe challenges to the safe and stable operation of electric power systems. Extensive researches have focused on the optimization of virtual power plants under uncertainties. Among these researches, stochastic optimization and robust optimization are two of the most popular methods. Reference [5] established an optimal stochastic scheduling model for virtual power plants considering the network security constraints and the wind speed uncertainty. Reference [6] formulated a three-stage stochastic optimization model for virtual power plants considering the uncertainties of the distributed energy resource production and load consumption. Reference [7] formulated the energy trading model of virtual power plants as a two-stage stochastic programming problem, in order to handle the uncertainty faced by virtual power plants. Reference [8] proposed a robust optimization approach for day-ahead resource scheduling of virtual power plants, accommodating the uncertainty of market prices, local demand, and renewable power output. Reference [9] proposed a day-ahead stochastic adaptive robust scheduling approach for virtual power plants with the uncertainty of wind power generation and electricity prices, which were modeled by confidence intervals and scenarios, respectively.

Distributionally robust optimization has become a new approach to handle uncertainty in recent years [10–12]. This method takes the probability distribution information of uncertain parameters (such as the moment information) into consideration and establishes an ambiguity set to contain all the possible probability distribution of uncertain parameters. Distributionally robust optimization combines the advantages of stochastic optimization and traditional robust optimization, and thus does not suffer the problem of sub-optimal solutions resulting from the over-dependence of stochastic optimization on the accurate probability distribution, as well as conservative results of traditional robust optimization because of neglecting probability distributions of uncertain parameters. Because of these advantages, distributionally robust optimization has been successfully applied in different fields of power systems, including unit commitment [13], optimal power flow [14], energy and reserve co-dispatch [15], and integrated energy systems [16]. Reference [17] studied a day-ahead unit commitment problem with stochastic wind power generations, where a distributionally robust optimization approach was employed to address wind power forecast errors. In this regard, the spatiotemporal correlation in wind power generations was captured appropriately. Reference [18] proposed a distributionally robust optimization method for real-time economic dispatch considering automatic generation control, which reduced the total cost of power generations and frequency regulation. Reference [19] developed a distributionally robust generation expansion planning model, so that the violation risk of operational limits arising from the uncertainties pertaining to wind power output was reduced.

In this paper, a distributionally robust optimization approach is employed to address the uncertainty of renewable power output for the day-ahead scheduling problem of virtual power plants. Firstly, a second-order cone-based ambiguity set that incorporates the first and second moments of renewable power output is constructed to make full use of the probability distribution information, and a day-ahead two-stage distributionally robust optimization model is proposed for virtual power plants. Then,

a solution method based on the affine policy and second-order cone duality theory is employed to equivalently reformulate the proposed model into a deterministic mixed-integer second-order cone programming problem, in which the affine policy is used to approximate the second-stage decision variables. Finally, a case study is employed to demonstrate the validity of the proposed model and solution method.

2 Distributionally Robust Optimal Dispatch Model of Virtual Power Plant

2.1 Ambiguity Set Definition

The ambiguity set covers all the possible probability distribution of renewable power output. In this study, the ambiguity set F is constructed with the predicted mean (first-order moment) and variance (second-order moment), expressed as the following matrix/vector form:

$$F = \left\{ \mathrm{P} \in P(\mathrm{R}^I) \;\middle|\; \begin{array}{c} \mathrm{P}[\boldsymbol{w} \in W] = 1 \\ \mathrm{E}_{\mathrm{P}}[\boldsymbol{w}] = \boldsymbol{\mu} \\ \mathrm{E}_{\mathrm{P}}[(\boldsymbol{w} - \boldsymbol{\mu})^2] \le \boldsymbol{\sigma} \end{array} \right\} \tag{1}$$

with

$$W = \left\{ \boldsymbol{w} \in \mathrm{R}^I \;\middle|\; \underline{\boldsymbol{w}} \le \boldsymbol{w} \le \bar{\boldsymbol{w}} \right\} \tag{2}$$

where $\boldsymbol{w}$ refers to the renewable power output $P_{w,t}^{\mathrm{RES}}$; F is the ambiguity set of $\boldsymbol{w}$; P is the probability distribution of $\boldsymbol{w}$; R stands for all possible probability distributions; I is the dimension of $\boldsymbol{w}$; $P(\mathrm{R}^I)$ refers to all possible probability distributions of $\boldsymbol{w}$; W means the uncertainty set of $\boldsymbol{w}$, which is expressed by Eq. (2); $\boldsymbol{\mu}$ and $\boldsymbol{\sigma}$ refer to the expected value and variance of $\boldsymbol{w}$, respectively; $\bar{\boldsymbol{w}}$ and $\underline{\boldsymbol{w}}$ indicate the upper and lower limits of $\boldsymbol{w}$, respectively.

In Eq. (1), the first line indicates that the values of renewable power output fall within its uncertainty set (2), which is similar to that of traditional robust optimization keeping the fluctuation of renewable power output within its upper and lower limits. The second line means that the expected value of renewable power output is equal to its predicted value, while the third line indicates that the variance of the renewable power output is within the range of its predicted variance. The expected value $\boldsymbol{\mu}$, the variance $\boldsymbol{\sigma}$, the upper limit $\bar{\boldsymbol{w}}$, and the lower limits $\underline{\boldsymbol{w}}$ of renewable power output are random variables, which can be obtained by history data statistics or probabilistic forecasting methods, while the renewable power output $\boldsymbol{w}$ is decision variables modeled by the ambiguity set.

In the ambiguity set (1), all the elements are in linear form except $(\boldsymbol{w} - \boldsymbol{\mu})^2$ in the third line. However, $(\boldsymbol{w} - \boldsymbol{\mu})^2$ could be easily transformed into a second-order cone program. Therefore, the ambiguity set F could be considered as a second-order cone program. Besides, the ambiguity set will degenerate into an uncertainty set if the probability distribution of renewable power output is not considered, and therefore the distributionally robust optimization approach will degenerate into a traditional robust optimization approach.

The square term in the ambiguity set makes the model difficult to be transformed and solved. To facilitate the transformation of the model, the auxiliary variable $\boldsymbol{v}$ is introduced to replace the square term $(\boldsymbol{w} - \boldsymbol{\mu})^2$ in the third line of the ambiguity set F, thus transforming F to the extended ambiguity set G:

$$G = \left\{ \mathrm{P} \in P(\mathrm{R}^{I \times I}) \;\middle|\; \begin{array}{c} \mathrm{P}[(\boldsymbol{w}, \boldsymbol{v}) \in \bar{W}] = 1 \\ \mathrm{E}_{\mathrm{P}}[\boldsymbol{w}] = \boldsymbol{\mu} \\ \mathrm{E}_{\mathrm{P}}[\boldsymbol{v}] \le \boldsymbol{\sigma} \end{array} \right\} \tag{3}$$

with

$$\bar{W} = \left\{ (\boldsymbol{w}, \boldsymbol{v}) \in \mathrm{R}^{I\times I} \;\middle|\; \begin{array}{c} \underline{\boldsymbol{w}} \le \boldsymbol{w} \le \bar{\boldsymbol{w}} \\ (\boldsymbol{w}-\boldsymbol{\mu})^2 \le \boldsymbol{v} \le \bar{\boldsymbol{v}} \end{array} \right\} \tag{4}$$

where $I \times I$ refers to the dimension of $(\boldsymbol{w}, \boldsymbol{v})$; W is the extended uncertainty set, which is defined in Eq. (4); $\bar{\boldsymbol{v}}$ refers to the upper limit of $\boldsymbol{v}$.

2.2 *Objective Function*

In this study, a basic virtual power plant, which includes gas turbines, renewable energy sources (including wind farms and photovoltaic arrays), and loads, are employed to explore the advantages of the distributionally robust optimization approach. The schematic of the virtual power plant studied in this paper is shown in Fig. 1.

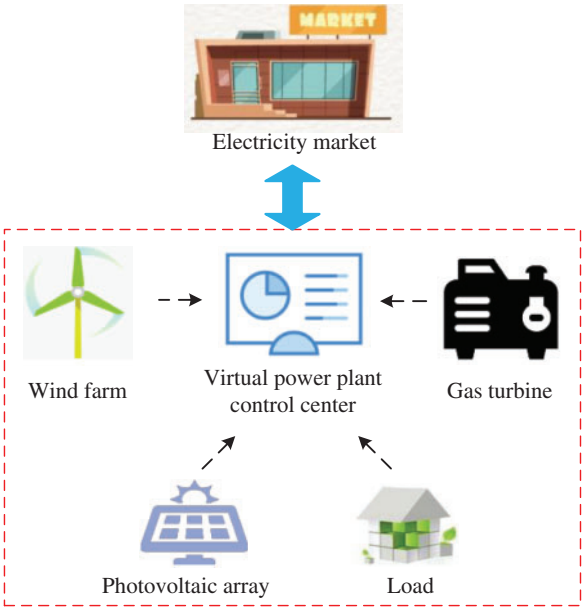

Figure 1: Schematic of studied virtual power plant

The distributionally robust formulation of virtual power plants corresponds to a two-stage optimization problem, in which the gas turbine unit commitment decisions and day-ahead bidding strategy in electricity markets are the first-stage decision variables. These decision variables should be decided one day ahead when the renewable power output is unknown. Other dispatch variables (including the gas turbine power output and power system dispatch decisions) are the second-stage decision variables, which are decided after renewable power output is realized. The objective function of the first stage model is expressed as:

$$\min_{x} \sum_{t}\sum_{e} \left(C_e^{\mathrm{SU}} u_{e,t} + C_e^{\mathrm{SD}} v_{e,t} + C_e^{\mathrm{NL}} x_{e,t}\right) - \sum_{t} \lambda_t^{\mathrm{EM}} P_t^{\mathrm{EM}} + \sup_{\mathrm{P}\in F} \mathrm{E}_{\mathrm{P}}\left[Q(\boldsymbol{x}, \boldsymbol{w})\right] \tag{5}$$

where t represents dispatch periods; e represents gas turbines; C_e^{SU}, C_e^{SD}, and C_e^{NL} refer to start-up, shut-down, and fixed costs of gas turbine e; Unit commitment variables $u_{e,t}$, $v_{e,t}$, and $x_{e,t}$ indicate whether gas turbine e is start-up, short-down, and on. If so, set at 1, otherwise, set at 0; λ_t^{EM} is the day-ahead market energy price; P_t^{EM} represents power traded (sold if positive or purchased if negative) in the day-ahead

market; $\boldsymbol{x} = \{x_{e,t}, u_{e,t}, v_{e,t}, P_t^{\mathrm{EM}}\}$ is the first-stage decision variable; $\mathrm{E_p}$ represents the expected value; $Q(\boldsymbol{x}, \boldsymbol{w})$ is the operation costs of the virtual power plant with given first-stage decision variables and renewable power output, which is the second-stage objective function expressed as follows:

$$Q(\boldsymbol{x}, \boldsymbol{w}) = \min_{\boldsymbol{y}} \sum_t \sum_e F_e^{\mathrm{GT}}(P_{e,t}^{\mathrm{GT}}) \tag{6}$$

where $F_e^{\mathrm{GT}}(\cdot)$ is the generation cost function of gas turbine e; $P_{e,t}^{\mathrm{GT}}$ refers to the active power output of gas turbine e. $\boldsymbol{y} = \{P_{e,t}^{\mathrm{GT}}, Q_{e,t}^{\mathrm{GT}}, P_{ij,t}, Q_{ij,t}, V_{i,t}\}$ is the second-stage decision variable, the meaning of each variable are detailed in the following session.

The power generation cost function of gas turbines is commonly a quadratic function, which can be linearized by the piecewise linearization method [20] as follows:

$$F_e^{\mathrm{GT}}(P_{e,t}^{\mathrm{GT}}) \geq b_{e,m} u_{e,t} + k_{e,m} P_{e,t}^{\mathrm{GT}} \tag{7}$$

where m is the number of pieces; $b_{e,m}$ and $k_{e,m}$ are the parameters of the linear function.

The first-stage objective function (5) consists of two parts. The first is the gas turbine unit commitment costs minus the virtual power plant revenue in the electricity market, while the second part is the expected value of the power generation cost of gas turbines calculated by Eq. (6) under the worst probability distribution of the renewable power output.

2.3 Constraint

The constraints of the first stage model state the relationship of binary variables of gas turbines:

$$x_{e,t} - x_{e,t-1} = u_{e,t} - v_{e,t} \tag{8}$$

$$x_{e,\tau} \geq u_{e,t} \quad \forall t \leq \tau \leq t + t_e^{\mathrm{U}} - 1 \tag{9}$$

$$1 - x_{e,\tau} \geq v_{e,t} \quad \forall t \leq \tau \leq t + t_e^{\mathrm{D}} - 1 \tag{10}$$

where t^{U} and t^{D} stand for the minimum start-up and shut-down time of gas turbine e, respectively.

Eq. (8) is the logical constraint of binary variables, while Eqs. (9) and (10) refer to the minimum start-up and shut-down time constraints of gas turbines.

The second-stage constraints include the gas turbine power output constraint and the distribution network constraint. It is worth mentioning that the distribution network constraint is taken into consideration here, in order to avoid power system problems such as bus voltage violation and branch overload.

The power output constraints of gas turbines can be expressed as follows:

$$\underline{P}_e^{\mathrm{GT}} x_{e,t} \leq P_{e,t}^{\mathrm{GT}} \leq \bar{P}_e^{\mathrm{GT}} x_{e,t} \tag{11}$$

$$\underline{Q}_e^{\mathrm{GT}} x_{e,t} \leq Q_{e,t}^{\mathrm{GT}} \leq \bar{Q}_e^{\mathrm{GT}} x_{e,t} \tag{12}$$

$$P_{e,t}^{\mathrm{GT}} - P_{e,t-1}^{\mathrm{GT}} \leq RU_e^{\mathrm{GT}} x_{e,t-1} + SU_e^{\mathrm{GT}} u_{e,t} \tag{13}$$

$$P_{e,t-1}^{\mathrm{GT}} - P_{e,t}^{\mathrm{GT}} \leq RD_e^{\mathrm{GT}} x_{e,t} + SD_e^{\mathrm{GT}} v_{e,t} \tag{14}$$

where $Q_{e,t}^{\mathrm{GT}}$ is the reactive power output of gas turbine e; RU_e^{GT} and RD_e^{GT} represent maximum ramp-up and ramp-down rates of gas turbine e, respectively; SU_e^{GT} and SD_e^{GT} stand for maximum power output when gas turbine e is start-up and shut-down.

Eqs. (11) and (12) are the upper and lower limits of the active and reactive power output of gas turbines, while Eqs. (13) and (14) stand for the ramp-up and ramp-down constraints of gas turbines.

The distribution network constraints is be described with the linearized DistFlow branch model [21]:

$$\sum_{e\in S_j^{\mathrm{GT}}} P_{e,t}^{\mathrm{GT}} + \sum_{w\in S_j^{\mathrm{RES}}} P_{w,t}^{\mathrm{RES}} + P_{ij,t} = \sum_{l\in S_j^{\mathrm{B,d}}} P_{jl,t} + P_{j,t}^{\mathrm{L}} + P_t^{\mathrm{EM}} \quad \forall j \in S^{\mathrm{PCC}} \tag{15}$$

$$\sum_{e\in S_j^{\mathrm{GT}}} P_{e,t}^{\mathrm{GT}} + \sum_{w\in S_j^{\mathrm{RES}}} P_{w,t}^{\mathrm{RES}} + P_{ij,t} = \sum_{l\in S_j^{\mathrm{B,d}}} P_{jl,t} + P_{j,t}^{\mathrm{L}} \quad \forall j \notin S^{\mathrm{PCC}} \tag{16}$$

$$\sum_{e\in S_j^{\mathrm{GT}}} Q_{e,t}^{\mathrm{GT}} + Q_{ij,t} = \sum_{l\in S_j^{\mathrm{B,d}}} Q_{jl,t} + Q_{j,t}^{\mathrm{L}} \tag{17}$$

$$V_{j,t} = V_{i,t} - \left(P_{ij,t} r_{ij} + Q_{ij,t} x_{ij}\right) / V^0 \tag{18}$$

$$-\bar{P}_{ij} \le P_{ij,t} \le \bar{P}_{ij} \tag{19}$$

$$-\bar{Q}_{ij} \le Q_{ij,t} \le \bar{Q}_{ij} \tag{20}$$

$$\underline{V}_i \le V_{i,t} \le \bar{V}_i \tag{21}$$

where w represents renewable energy units; i, j, and l stand for buses; S_j^{GT} and S_j^{RES} are the gas turbine and renewable energy unit set at bus j; $S_j^{\mathrm{B,d}}$ is the set of downstream buses connecting to bus j; S^{PCC} is the set of connection points between the distribution and main networks; $P_{w,t}^{\mathrm{RES}}$ is the power output of the renewable energy unit w. $P_{ij,t}$ and $Q_{ij,t}$ refer to active and reactive power flow of branch i-j, respectively; $P_{i,t}^{L}$ and $Q_{i,t}^{L}$ are active and reactive loads of bus i, respectively; $V_{i,t}$ is voltage magnitude of bus i; r_{ij} and x_{ij} stand for resistance and reactance of branch i-j, respectively; V^0 is voltage magnitude at the slack bus.

Eqs. (15) and (16) indicate active power balance constraints. Eq. (17) represents reactive power balance constraint. Eq. (18) refers to the relation between nodal voltage magnitudes and branch power flows. Eqs. (19)–(21) stand for the upper and lower limits for active branch power flow, reactive branch power flow, and bus voltage magnitudes.

3 Solution Method

3.1 Affine Policy

The distributionally robust optimization model is a typical NP-hard problem, for which the optimal solution of the second-stage decision variables cannot be found until traversing all realizations of uncertain parameters. The affine policy can effectively overcome this computational obstacle. Under the policy, the second-stage decision variables affinely depend on uncertain parameters. In order to match with the extended ambiguity set G, the decision variable y in the second stage is constrained to be an affine function of the uncertain variable $\boldsymbol{w}$ and the auxiliary variable $\boldsymbol{v}$, which is expressed as follows:

$$\boldsymbol{y}(\boldsymbol{w}, \boldsymbol{v}) = \boldsymbol{y}_0 + \boldsymbol{Y}_{\mathrm{w}}\boldsymbol{w} + \boldsymbol{Y}_{\mathrm{v}}\boldsymbol{v} \tag{22}$$

where $\boldsymbol{y}_0$, $\boldsymbol{Y}_{\mathrm{w}}$, and $\boldsymbol{Y}_{\mathrm{v}}$ are linear coefficients of the affine function, representing the decision variables.

Taking $P_{e,t}^{\mathrm{GT}}$ as an example, the linear affine function is represented as:

$$P_{e,t}^{\mathrm{GT}}(w_{w,t}, v_{w,t}) = P_{e,t}^{\mathrm{GT},0} + \sum_{w} P_{e,w,t}^{\mathrm{GT,w}} w_{w,t} + \sum_{w} P_{e,w,t}^{\mathrm{GT,v}} v_{w,t} \tag{23}$$

The linear affine functions of other second-stage decision variables (including $Q_{e,t}^{\mathrm{GT}}$, $P_{ij,t}$, $Q_{ij,t}$, and $V_{i,t}$) are similar as that of $P_{e,t}^{\mathrm{GT}}$, and are omitted here due to the space limitation.

3.2 Abstract Formulation

For notational brevity, the day-ahead distributionally robust optimization model of virtual power plants is represented as the following matrix/vector form:

$$\min_{x} \ \boldsymbol{c}^T \boldsymbol{x} + \sup_{\mathrm{P}\in G} \mathrm{E}_{\mathrm{P}}[Q(\boldsymbol{x}, \boldsymbol{w})] \tag{24}$$

$$\text{s.t.} \ \ \boldsymbol{A}\boldsymbol{x} \le \boldsymbol{b} \tag{25}$$

with

$$Q(\boldsymbol{x}, \boldsymbol{w}) = \min_{y} \boldsymbol{d}^T \boldsymbol{y} \tag{26}$$

$$\text{s.t.} \ \ \boldsymbol{E}\boldsymbol{x} + \boldsymbol{G}\boldsymbol{y} + \boldsymbol{M}\boldsymbol{w} \le \boldsymbol{h} \tag{27}$$

where $\boldsymbol{A}$, $\boldsymbol{E}$, $\boldsymbol{G}$, $\boldsymbol{M}$, $\boldsymbol{b}$, $\boldsymbol{c}$, $\boldsymbol{d}$, and $\boldsymbol{h}$ are coefficient matrices and vectors of the optimization model.

Eqs. (24) and (25) are the matrix/vector forms of the objective function and constraints in the first stage, respectively; Eqs. (26) and (27) are the matrix/vector forms of the objective function and constraints in the second stage, respectively. It should be noted that in Eq. (24), the ambiguity set F has been replaced by the extended ambiguity set G.

3.3 Model Reformulation

The supremum (sup) problem in the objective function (24), which is an infinite-dimensional problem, is difficult to solve. To deal with this, we first express the supremum problem as the following semi-infinite optimization problem, according to the definition of the extended ambiguity set G(3):

$$\sup_{\mathrm{P}\in G} \mathrm{E}_{\mathrm{P}}[Q(\boldsymbol{x}, \boldsymbol{w})] = \max \int_{\tilde{W}} \boldsymbol{d}^T \boldsymbol{y}(\boldsymbol{w}, \boldsymbol{v}) \, df(\boldsymbol{w}, \boldsymbol{v}) \tag{28}$$

$$\text{s.t.} \ \int_{\tilde{W}} df(\boldsymbol{w}, \boldsymbol{v}) = 1 \quad : \alpha \tag{29}$$

$$\int_{\tilde{W}} \boldsymbol{w} df(\boldsymbol{w}, \boldsymbol{v}) = \boldsymbol{\mu} \quad : \boldsymbol{\beta} \tag{30}$$

$$\int_{\tilde{W}} \boldsymbol{v} df(\boldsymbol{w}, \boldsymbol{v}) \le \boldsymbol{\sigma} \quad : \boldsymbol{\gamma} \tag{31}$$

$$f(\boldsymbol{w}, \boldsymbol{v}) \ge 0 \tag{32}$$

where $f(\boldsymbol{w}, \boldsymbol{v})$ is the joint probability density function of $\boldsymbol{w}$ and $\boldsymbol{v}$; α, $\boldsymbol{\beta}$, and $\boldsymbol{\gamma}$ are dual variables of the constraint Eqs. (29)–(31), respectively.

Eqs. (29)–(31) correspond to the formulas in the first to third lines in the ambiguity set G(3); Eq. (32) highlights the non-negativity of $f(\boldsymbol{w}, \boldsymbol{v})$.

Then, the strong duality theory is applied to transform the semi-infinite optimization problem (28)–(32) to a finite-dimensional dual problem. Replacing the supremum problem in the original

problem (24)–(27) with the obtained finite-dimensional dual problem, we can have the equivalent form of the original problem as follows:

$$\min \ \boldsymbol{c}^T\boldsymbol{x}+\alpha+\boldsymbol{\beta}^T\boldsymbol{\mu}+\boldsymbol{\gamma}^T\boldsymbol{\sigma} \tag{33}$$

$$\text{s.t. } \boldsymbol{A}\boldsymbol{x}\le\boldsymbol{b} \tag{34}$$

$$\boldsymbol{\gamma}\ge\boldsymbol{0} \tag{35}$$

$$\alpha+\boldsymbol{\beta}^T\boldsymbol{w}+\boldsymbol{\gamma}^T\boldsymbol{v}\ge\boldsymbol{d}^T\boldsymbol{y}(\boldsymbol{w},\boldsymbol{v})\ \ \forall(\boldsymbol{w},\boldsymbol{v})\in\bar{W} \tag{36}$$

$$\boldsymbol{E}\boldsymbol{x}+\boldsymbol{G}\boldsymbol{y}(\boldsymbol{w},\boldsymbol{v})+\boldsymbol{M}\boldsymbol{w}\le\boldsymbol{h}\ \ \forall(\boldsymbol{w},\boldsymbol{v})\in\bar{W} \tag{37}$$

Finally, the second-order cone duality theory is used to convert the robust constraints (36) and (37) into their dual problems (see Appendix A for detailed conversion processes), and the final form of the distributionally robust optimization model can be expressed as follows:

$$\min \ \boldsymbol{c}^T\boldsymbol{x}+\alpha+\boldsymbol{\beta}^T\boldsymbol{\mu}+\boldsymbol{\gamma}^T\boldsymbol{\sigma} \tag{38}$$

$$\text{s.t. } \boldsymbol{A}\boldsymbol{x}\le\boldsymbol{b} \tag{39}$$

$$\boldsymbol{\gamma}\ge\boldsymbol{0} \tag{40}$$

$$\alpha-\boldsymbol{d}^T\boldsymbol{y}_0\ge\underline{\boldsymbol{w}}^T\boldsymbol{\delta}+\bar{\boldsymbol{w}}^T\boldsymbol{\varepsilon}-2\boldsymbol{\mu}^T\boldsymbol{\eta}-\boldsymbol{1}^T\boldsymbol{\kappa}+\boldsymbol{1}^T\boldsymbol{\pi}+\bar{\boldsymbol{v}}^T\boldsymbol{\rho} \tag{41}$$

$$\boldsymbol{\delta}+\boldsymbol{\varepsilon}-2\boldsymbol{\eta}=\boldsymbol{Y}_{\mathrm{w}}^T\boldsymbol{d}-\boldsymbol{\beta} \tag{42}$$

$$-\boldsymbol{\kappa}-\boldsymbol{\pi}+\boldsymbol{\rho}=\boldsymbol{Y}_{\mathrm{v}}^T\boldsymbol{d}-\boldsymbol{\gamma} \tag{43}$$

$$\left\|\begin{matrix}\boldsymbol{\eta}\\ \boldsymbol{\kappa}\end{matrix}\right\|\le\boldsymbol{\pi} \tag{44}$$

$$\boldsymbol{\delta}\le 0,\boldsymbol{\varepsilon}\ge 0,\boldsymbol{\rho}\ge 0 \tag{45}$$

$$\left(\boldsymbol{h}-\boldsymbol{E}\boldsymbol{x}-\boldsymbol{G}\boldsymbol{y}_0\right)_k\ge\underline{\boldsymbol{w}}^T\boldsymbol{\delta}_k+\bar{\boldsymbol{w}}^T\boldsymbol{\varepsilon}_k-2\boldsymbol{\mu}^T\boldsymbol{\eta}_k-\boldsymbol{1}^T\boldsymbol{\kappa}_k+\boldsymbol{1}^T\boldsymbol{\pi}_k+\bar{\boldsymbol{v}}^T\boldsymbol{\rho}_k \tag{46}$$

$$\boldsymbol{\delta}_k+\boldsymbol{\varepsilon}_k-2\boldsymbol{\eta}_k=(\boldsymbol{G}\boldsymbol{Y}_{\mathrm{w}}+\boldsymbol{M})_k^T \tag{47}$$

$$-\boldsymbol{\kappa}_k-\boldsymbol{\pi}_k+\boldsymbol{\rho}_k=(\boldsymbol{G}\boldsymbol{Y}_{\mathrm{v}})_k^T \tag{48}$$

$$\left\|\begin{matrix}\boldsymbol{\eta}_k\\ \boldsymbol{\kappa}_k\end{matrix}\right\|\le\boldsymbol{\pi}_k \tag{49}$$

$$\boldsymbol{\delta}_k\le 0,\boldsymbol{\varepsilon}_k\ge 0,\boldsymbol{\rho}_k\ge 0 \tag{50}$$

where $\boldsymbol{\delta},\boldsymbol{\varepsilon},\boldsymbol{\eta},\boldsymbol{\kappa},\boldsymbol{\pi},\boldsymbol{\rho}$ are the dual variables deriving from the dual transformation of robust constraint (36); $\boldsymbol{1}$ is the vector with all elements being 1; $(\cdot)_k$ represents the k^{th} row of the matrix/vector; $\boldsymbol{\delta}_k,\boldsymbol{\varepsilon}_k,\boldsymbol{\eta}_k,\boldsymbol{\kappa}_k,\boldsymbol{\pi}_k,\boldsymbol{\rho}_k$ are the dual variables deriving from the dual transformation of the k^{th} constraint of (37).

In this way, the original distributionally robust optimization model (24)–(27) can be equivalently transformed into the deterministic mixed-integer second-order cone programming problem (38)–(50).

4 Case Study

4.1 Test System Description

A virtual power plant composed of three gas turbines, one wind farm, one photovoltaic array, and loads in the distribution network is tested here. The parameters of gas turbines are shown in

Table B1, Appendix B. The wind farm is assumed to include two 1.5-MW wind turbines (Goldwind GW 77/1500 [22]), whose cut-in, cut-out, and rated wind speeds are 3, 22, and 11 m/s, respectively, and fitting coefficients are $a_0 = 0.50$, $a_1 = -0.31$, $a_2 = 0.059$, $a_3 = -0.0025$. The photoelectric transformation efficiency of the photovoltaic array is 15.7% [23] and the total surface area of the photovoltaic array is 25000 m^2. Historical data of wind speed and solar irradiance for Jan. 2021 [24] are used to calculate expected values of wind and photovoltaic power output (see Appendix C for detailed calculation processes). The expected values of wind power output, photovoltaic power output, and loads are shown in Fig. B1, Appendix B. The IEEE 33-bus distribution system is considered here and its structure is shown in Fig. 2. The three gas turbines, wind farm, and photovoltaic array are located at nodes 22, 18, 33, 12, and 25, respectively. The parameters of the IEEE 33-bus system can be found in [25]. The electricity market price [26] is shown in Fig. B2, Appendix B. The commercial solver MOSEK in the GAMS platform is used to solve finally mixed-integer second-order cone programming problem, with the relative gap set to 0.1%.

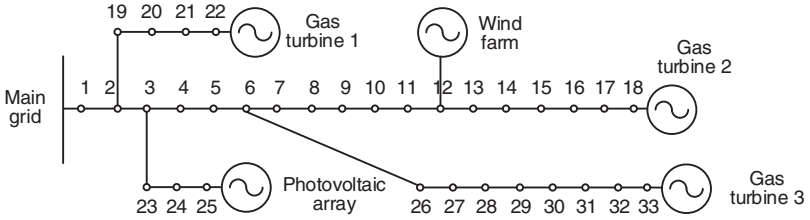

Figure 2: IEEE 33-bus distribution test system

4.2 Comparison with Different Optimization Approaches

1) Optimization results

The proposed distributionally robust optimization approach is compared with the stochastic optimization and traditional robust optimization approaches. The relative standard deviation (obtained by $\sqrt{\gamma}/\mu$) of the stochastic and distributionally robust optimization model is set to 0.3 [27]. In order to generate scenarios of renewable power output for the stochastic optimization approach, we assume that renewable power output follows Gaussian distribution and use the Monte Carlo method to generate 5000 initial scenarios of renewable power output according to the expected value and relative standard deviation. Then, the scenario reduction method (see Appendix D for detailed illustrations and steps) is applied to reduce 5000 initial scenarios to 500 representative scenarios. As for the robust optimization approach, the upper and lower limits of renewable power output are employed for solving the model.

The traded energy (sold if positive or purchased if negative) of the virtual power plant in electricity markets and costs for the three optimization approaches are shown in Fig. 3 and Table 1, respectively.

The stochastic, traditional robust, and distributionally robust optimization approaches focus on the expected distribution, the worst-case distribution, and the worst-case of uncertainties, respectively. As such, the decisions of the stochastic optimization approach are most radical among these three methods, expressed as the virtual power plant tends to sell more energy and purchase less energy in electricity markets, which can be observed in Fig. 3. Such a strategy can obtain a lower total cost under ideal conditions where probability distributions of renewable power output are estimated precisely (see Table 1). However, less energy purchased may bring serious load shedding problems to the virtual power plant under a few unforeseen scenarios with low renewable power output (detailed

analyses can be found below). The traditional robust optimization approach, in contrast, is the most conservative method, in which the virtual power plant tends to sell less energy and purchase more energy. This conservative strategy yields a relatively high total cost. The distributionally robust optimization approach can mitigate the over-conservative problem of the traditional one by further capturing the distribution information of renewable power output, which finally reduces the total cost of the virtual power plant by 31.39%.

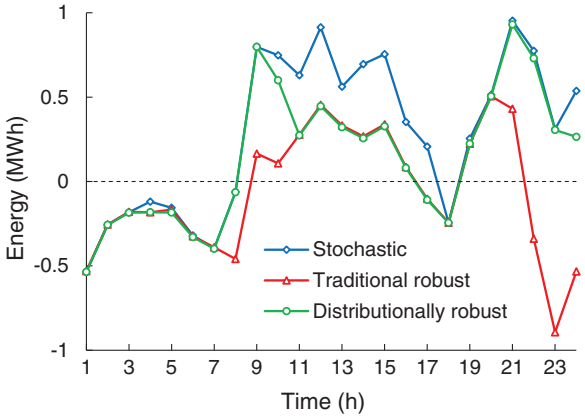

Figure 3: Traded energy for different optimization approaches

Table 1: Costs for different optimization approaches

Optimization approach	Gas turbine cost	Electricity market revenue	Total cost
Stochastic	1015.07	199.54	815.53
Traditional robust	1225.07	−12.48	1237.55
Distributionally robust	961.59	112.51	849.08

We further test the performance of stochastic, traditional robust, and distributionally robust optimization approaches by out-of-sample analyses. In order to do this, we first solve the three models to obtain the first-stage decision variables (i.e., the gas turbine unit commitment decisions and day-ahead bidding strategy), and then solve the second-stage model for the given first-stage decision variables under 500 out-of-sample scenarios. Note that the solution results of the stochastic optimization approach in Table 1 are obtained under the predetermined distribution (i.e., the Gaussian distribution). However, the actual probability distribution is normally different from the predetermined distribution because of estimation or forecast errors. In this regard, load shedding may emerge in the virtual power plant when a few unforeseen scenarios occur in practice. For ensuring the solvability under all out-of-sample scenarios, we further add a load shedding variable in the power balance constraint (15), and the product of the load shedding variable and a penalty cost (4000 $/MWh [28]) in the objective function (5).

The expected load shedding and total cost for the three approaches under a discrepant distribution (uniform distribution as a comparative example) are listed in Table 2. We can see that the stochastic optimization method suffers serious load shedding problems in this case with inaccurate estimations of probability distributions. This problem, however, is effectively avoided in the distributionally robust

optimization approach, because descriptive statistics instead of detailed probability distributions are employed to cover the vagueness of the distribution information in this approach.

Table 2: Expected load shedding and total costs for different optimization approaches

Optimization approach	Expected load shedding coast	Expected total cost
Stochastic	169.40	990.43
Traditional robust	0	878.67
Distributionally robust	0	850.49

Generally, the distributionally robust optimization approach is the intermediation of the stochastic and traditional robust approach, which can guarantee a relatively low total cost and prevent serious load shedding simultaneously. That is, the distributionally robust optimization approach represents a good trade-off between robustness and economy, and thus should be favored by virtual power plant operators.

2) Computational times

The computational times for stochastic optimization, robust optimization, and distributionally robust optimization models are shown in Table 3. The stochastic optimization approach suffers from a large computational burden because of scenario enumerations. By comparison, the calculation time of the distributionally robust optimization approach is reduced by 80.95%, since heavy calculations arising from scenario enumerations are avoided. Besides, the computational time of the distributionally robust optimization model is less than 20 s, which is much less than the time threshold of the day-ahead dispatch problem. This is because the proposed solution method converts the complex distributionally optimization model into a deterministic mixed-integer second-order cone programming problem, and thereby greatly reducing the difficulty of model solving. This verifies the effectiveness of the proposed solution method.

Table 3: Computational times for different optimization approaches

Optimization approach	Computation time (s)
Stochastic	90.52
Traditional robust	1.58
Distributionally robust	17.24

4.3 Performance of Moment

The moment information of renewable power output is incorporated in the ambiguity set to depict its probability distribution features. This section explores the impact of the moment information on the optimization results. Here, the relative standard deviation is used to reflect the change of the variance. The total traded energy in the electricity market and the objective function value (total cost) of the virtual power plant as shown in Fig. 4, after solving the robust optimization model under different relative standard deviations.

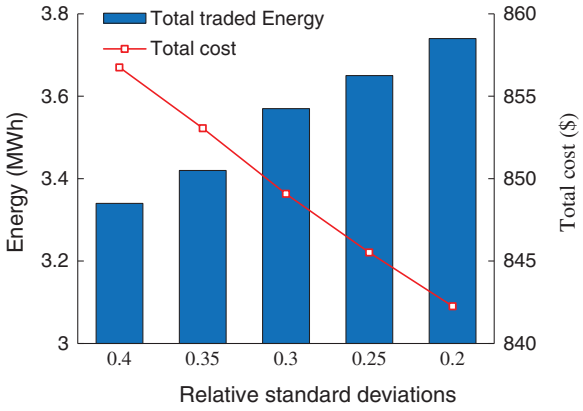

Figure 4: Traded energy and objective functions with different relative standard deviations

The traded energy of the virtual power plant in the electricity market gradually increases with the decreasing relative standard deviation. This is because the decreasing of the relative standard deviation means that the decreased fluctuation of the renewable power output. In this regard, the virtual power plant only needs to buy less energy (or sell more energy) in electricity markets to cope with the risks caused by the fluctuation of renewable power output, which reduces the total cost of the virtual power plant. This means that the adaptability of the dispatch strategy to the fluctuation of renewable power output is improved in the distributionally robust optimization approach. That is, the distributionally robust optimization approach enables the operator to adjust the dispatch strategy based on the moment information of the renewable power output so as to reduce the total cost. This adjustment capability cannot be achieved in the traditional robust optimization approach.

5 Conclusions

In this study, we consider the impact of the uncertainty of renewable power output on virtual power plant dispatch, and propose a day-ahead distributionally robust optimization dispatch model for the virtual power plant. The solution results show that:

1) Compared with stochastic and traditional robust optimization methods, the proposed distributionally robust optimization method can better balance the robustness and economy of dispatch decisions.
2) The proposed distributionally robust optimization approach can adjust the dispatch strategy of the virtual power plant according to the moment information of the renewable power output, and thus the total cost of the virtual power plant is reduced.
3) The solve difficulty of the distributionally robust optimization model is effectively reduced by the proposed solution method, which results in that the proposed model can be solved in a short time.

Funding Statement: This work was supported by the Technology Project of State Grid Jiangsu Electric Power Co., Ltd., China, under Grant J2020090.

Conflicts of Interest: The authors declare that they have no conflicts of interest to report regarding the present study.

References

1. Naval, N., Yusta, J. M. (2021). Virtual power plant models and electricity markets–A review. *Renewable & Sustainable Energy Reviews, 149,* 1–13. DOI 10.1016/j.rser.2021.111393.
2. Nosratabadi, S. M., Hooshmand, R. A., Gholipour, E. (2017). A comprehensive review on microgrid and virtual power plant concepts employed for distributed energy resources scheduling in power systems. *Renewable & Sustainable Energy Reviews, 67,* 341–363. DOI 10.1016/j.rser.2016.09.025.
3. Zhou, Y., Wei, Z., Sun, G., Cheung, K. W., Zang, H. et al. (2019). Four-level robust model for a virtual power plant in energy and reserve markets. *IET Generation, Transmission & Distribution, 13(11),* 2036–2043. DOI 10.1049/iet-gtd.2018.5197.
4. Yi, Z., Xu, Y., Wang, H., Sang, L. (2021). Coordinated operation strategy for a virtual power plant with multiple DER aggregators. *IEEE Transactions on Sustainable Energy, 12(4),* 2445–2458. DOI 10.1109/TSTE.2021.3100088.
5. Rahimia, M., Ardakania, F. Z., Ardakanib, A. J. (2021). Optimal stochastic scheduling of electrical and thermal renewable and non-renewable resources in virtual power plant. *International Journal of Electrical Power & Energy Systems, 127,* 1–19. DOI 10.1016/j.ijepes.2020.106658.
6. Kardakos, E. G., Simoglou, C. K., Bakirtzis, A. G. (2016). Optimal offering strategy of a virtual power plant: A stochastic bi-level approach. *IEEE Transactions on Smart Grid, 7(2),* 794–806. DOI 10.1109/TSG.2015.2419714.
7. Shabanzadeh, M., Sheikh-El-Eslami, M. K., Haghifam, M. R. (2017). Risk-based medium-term trading strategy for a virtual power plant with first-order stochastic dominance constraints. *IET Generation, Transmission & Distribution, 11(2),* 520–529. DOI 10.1049/iet-gtd.2016.1072.
8. Naughton, J., Wang, H., Cantoni, M., Mancarella, P. (2021). Co-optimizing virtual power plant services under uncertainty: A robust scheduling and receding horizon dispatch approach. *IEEE Transactions on Power Systems, 36(5),* 3960–3972. DOI 10.1109/TPWRS.2021.3062582.
9. Baringo, A., Baringo, L., Arroyo, M. (2019). Day-ahead self-scheduling of a virtual power plant in energy and reserve electricity markets under uncertainty. *IEEE Transactions on Power Systems, 34(3),* 1881–1894. DOI 10.1109/TPWRS.59.
10. Bertsimas, D., Sim, M., Zhang, M. (2018). Adaptive distributionally robust optimization. *Management Science, 65(2),* 1–30. DOI 10.1287/mnsc.2017.2952.
11. Delage, E., Ye, Y. (2010). Distributionally robust optimization under moment uncertainty with application to data-driven problems. *Operations Research, 58(3),* 595–612. DOI 10.1287/opre.1090.0741.
12. Wiesemann, W., Kuhn, D., Sim, M. (2014). Distributionally robust convex optimization. *Operations Research, 62(6),* 1358–1376. DOI 10.1287/opre.2014.1314.
13. Xiong, P., Jirutitijaroen, P., Singh, C. (2017). A distributionally robust optimization model for unit commitment considering uncertain wind power generation. *IEEE Transactions on Power Systems, 32(1),* 39–49. DOI 10.1109/TPWRS.2016.2544795.
14. Zhang, Y., Shen, S., Mathieu, J. L. (2017). Distributionally robust chance-constrained optimal power flow with uncertain renewables and uncertain reserves provided by loads. *IEEE Transactions on Power Systems, 32(2),* 1378–1388. DOI 10.1109/TPWRS.2016.2572104.
15. Wei, W., Liu, F., Mei, S. (2016). Distributionally robust co-optimization of energy and reserve dispatch. *IEEE Transactions on Sustainable Energy, 7(1),* 289–300. DOI 10.1109/TSTE.2015.2494010.
16. Zhou, Y., Shahidehpour, M., Wei, Z., Li, Z., Sun, G. et al. (2020). Distributionally robust unit commitment in coordinated electricity and district heating networks. *IEEE Transactions on Power Systems, 35(3),* 2155–2166. DOI 10.1109/TPWRS.59.
17. Zheng, X., Qu, K., Lv, J., Li, Z., Zeng, B. (2021). Addressing the conditional and correlated wind power forecast errors in unit commitment by distributionally robust optimization. *IEEE Transactions on Sustainable Energy, 12(2),* 944–954. DOI 10.1109/TSTE.2020.3026370.

18. Liu, L., Hu, Z., Duan, X., Pathak, N. (2021). Data-driven distributionally robust optimization for real-time economic dispatch considering secondary frequency regulation cost. *IEEE Transactions on Power Systems, 36(5),* 4172–4184. DOI 10.1109/TPWRS.2021.3056390.
19. Pourahmadi, F., Kazempour, J. (2021). Distributionally robust generation expansion planning with unimodality and risk constraints. *IEEE Transactions on Power Systems, 36(5),* 4281–4295. DOI 10.1109/TPWRS.2021.3057265.
20. Zhao, C., Guang, Y. (2013). Unified stochastic and robust unit commitment. *IEEE Transactions on Power Systems, 28(3),* 3353–3361. DOI 10.1109/TPWRS.59.
21. Yeh, H., Gayme, D. F., Low, S. H. (2012). Adaptive VAR control for distribution circuits with photovoltaic generators. *IEEE Transactions on Power Systems, 27(3),* 1656–1663. DOI 10.1109/TPWRS.2012.2183151.
22. Goldwind GW 77/1500 (2021). https://en.wind-turbine-models.com/turbines/106-goldwind-gw-77-1500.
23. Yang, H., Xiong, T., Qiu, J., Qiu, D., Dong, Z. Y. (2016). Optimal operation of DES/CCHP based regional multi-energy prosumer with demand response. *Applied Energy, 167,* 353–565. DOI 10.1016/j.apenergy.2015.11.022.
24. NREL Flatirons Campus (M2) (2021). https://midcdmz.nrel.gov/apps/sitehome.pl?site=NWTC#.
25. Baran, M. E., Wu, F. F. (1989). Network reconfiguration in distribution systems for loss reduction and load balancing. *IEEE Transactions on Power Systems, 4(2),* 1401–1407. DOI 10.1109/61.25627.
26. PJM-Markets & Operations (2021). http://www.pjm.com/markets-and-operations.aspx.
27. Hong, Y. Y., Satriani, T. R. A. (2020). Day-ahead spatiotemporal wind speed forecasting using robust design-based deep learning neural network. *Energy, 209,* 1–13. DOI 10.1016/j.energy.2020.118441.
28. Zamani, A. G., Zakariazadeh, A., Jadid, S. (2016). Day-ahead resource scheduling of a renewable energy based virtual power plant. *Applied Energy, 169,* 324–340. DOI 10.1016/j.apenergy.2016.02.011.

Appendix A

This appendix provides the transformation from robust constraint (36) to (41)–(45). Robust constraints (37) can also be transformed into (46)–(50) by a similar process. Put affine function (22) into robust constraint (36), we obtain:

$$\alpha + \boldsymbol{\beta}^T \boldsymbol{w} + \boldsymbol{\gamma}^T \boldsymbol{v} \geq \boldsymbol{d}^T (\boldsymbol{y}_0 + \boldsymbol{Y}_{\mathrm{w}} \boldsymbol{w} + \boldsymbol{Y}_{\mathrm{v}} \boldsymbol{v}) \quad \forall (\boldsymbol{w}, \boldsymbol{v}) \in \bar{W} \tag{A1}$$

Then, (A1) is rewritten into the following equation under the worst scenario:

$$\alpha - \boldsymbol{d}^T \boldsymbol{y}_0 \geq \max_{(\boldsymbol{w},\boldsymbol{v}) \in \bar{W}} \left[\left(\boldsymbol{Y}_w^T \boldsymbol{d} - \boldsymbol{\beta} \right)^T \boldsymbol{w} + \left(\boldsymbol{Y}_v^T \boldsymbol{d} - \boldsymbol{\gamma} \right)^T \boldsymbol{v} \right] \tag{A2}$$

In (A2), the uncertain variable $\boldsymbol{w}$ and auxiliary variable $\boldsymbol{v}$ are within the constraints of the extended uncertainty set $\bar{W}$ (4), in which all elements are linear constraints except for $(\boldsymbol{w} - \boldsymbol{\mu})^2 \leq \boldsymbol{v}$. Rewrite the $(\boldsymbol{w} - \boldsymbol{\mu})^2 \leq \boldsymbol{v}$ into the following second-order cone form:

$$\left\| \begin{matrix} 2(\boldsymbol{w} - \boldsymbol{\mu}) \\ \boldsymbol{v} - \mathbf{1} \end{matrix} \right\| \leq \boldsymbol{v} + \mathbf{1} \tag{A3}$$

Introduce the auxiliary variables $\boldsymbol{\tau}$, $\boldsymbol{\psi}$, $\boldsymbol{\zeta}$ into the set $\bar{W}$ (4) and we have the constraints of the set (4) as:

$$\boldsymbol{w} \geq \underline{\boldsymbol{w}} : \boldsymbol{\delta} \tag{A4}$$

$$\boldsymbol{w} \leq \bar{\boldsymbol{w}} : \boldsymbol{\varepsilon} \tag{A5}$$

$$2(\boldsymbol{w} - \boldsymbol{\mu}) = \boldsymbol{\tau} : \boldsymbol{\eta} \tag{A6}$$

$$\boldsymbol{v} - \mathbf{1} = \boldsymbol{\psi} : \boldsymbol{\kappa} \tag{A7}$$

$$\boldsymbol{v} + \mathbf{1} = \boldsymbol{\zeta} : \boldsymbol{\pi} \tag{A8}$$

$$\left\| \begin{matrix} \boldsymbol{\tau} \\ \boldsymbol{\psi} \end{matrix} \right\| \leq \boldsymbol{\zeta} : \boldsymbol{\theta} \tag{A9}$$

$$\boldsymbol{v} \leq \bar{\boldsymbol{v}} : \boldsymbol{\rho} \tag{A10}$$

where $\boldsymbol{\delta}$, $\boldsymbol{\varepsilon}$, $\boldsymbol{\eta}$, $\boldsymbol{\kappa}$, $\boldsymbol{\pi}$, $\boldsymbol{\theta}$, $\boldsymbol{\rho}$ are the dual variables of the corresponding constraint formula; $\mathbf{1}$ means a vector with all elements being 1.

It is worth mentioning that the constraint Eqs. (A6)–(A9) collectively represent the constraint Eq. (A3), i.e., $(\boldsymbol{w} - \boldsymbol{\mu})^2 \leq \boldsymbol{v}$ in the extended ambiguity set $\bar{W}$.

Eq. (A2) satisfies the constraints (A4)–(A10). Thus, (A2) can be transformed into the following dual problem using the second-order cone duality theory:

$$\alpha - \boldsymbol{d}^T \boldsymbol{y}_0 \geq \underline{\boldsymbol{w}}^T \boldsymbol{\delta} + \bar{\boldsymbol{w}}^T \boldsymbol{\varepsilon} - 2\boldsymbol{\mu}^T \boldsymbol{\eta} - \mathbf{1}^T \boldsymbol{\kappa} + \mathbf{1}^T \boldsymbol{\pi} + \bar{\boldsymbol{v}}^T \boldsymbol{\rho} \tag{A11}$$

$$\boldsymbol{\delta} + \boldsymbol{\varepsilon} - 2\boldsymbol{\eta} = \boldsymbol{Y}_{\mathrm{w}}^T \boldsymbol{d} - \boldsymbol{\beta} \tag{A12}$$

$$-\boldsymbol{\kappa} - \boldsymbol{\pi} + \boldsymbol{\rho} = \boldsymbol{Y}_{\mathrm{v}}^T \boldsymbol{d} - \boldsymbol{\gamma} \tag{A13}$$

$$\left\| \begin{matrix} \boldsymbol{\eta} \\ \boldsymbol{\kappa} \end{matrix} \right\| \leq \boldsymbol{\pi} \tag{A14}$$

$$\boldsymbol{\delta} \leq 0, \boldsymbol{\varepsilon} \geq 0, \boldsymbol{\rho} \geq 0 \tag{A15}$$

Appendix B

Table B1: Parameters of gas turbines

No.	Start-up/Shut-down costs ($)	Fixed cost ($/h)	Maximum/ Minimum active power output (MW)	Maximum/ Minimum reactive power output (MVar)	First-/ Second-piece generation cost slope ($/MWh)
Unit 1	3/3	325.69	1.2/0.2	1/−1	12/16
Unit 2	2/2	−217.83	0.8/0.3	0.65/−0.65	15/20
Unit 3	1/1	206.16	1.4/0.4	1.1/−1.1	21/28

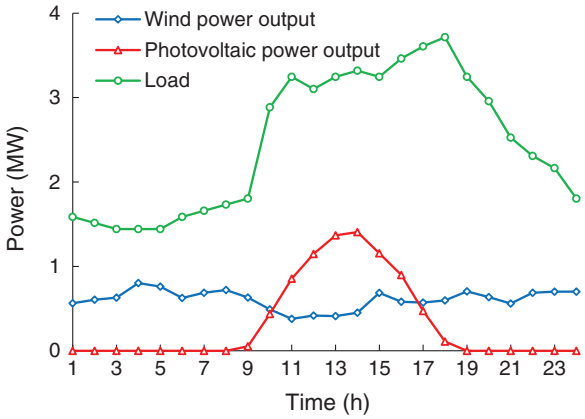

Figure B1: Expected values of wind power output, photovoltaic power output, and loads

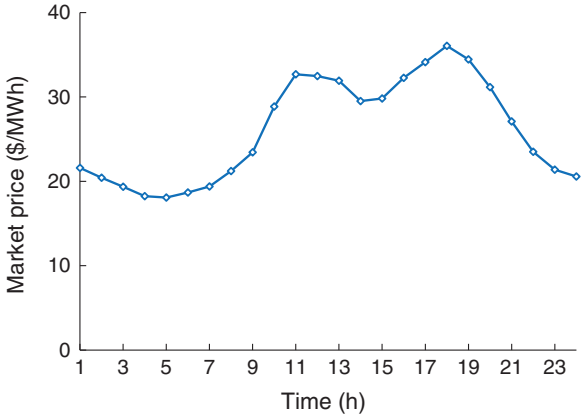

Figure B2: Electricity market prices

Appendix C

This appendix provides the calculation steps of expected values of wind and photovoltaic power output, which are illustrated as follows:

Step 1: Expected values of wind speed and solar irradiance are calculated by their historical data for January 2021.

Step 2: Wind power output is calculated by wind speed according to the wind power conversion curve:

$$P_{w,t}^{\mathrm{W}} = \begin{cases} 0, & v_{w,t} < v_w^{\mathrm{CI}},\ v_{w,t} > v_w^{\mathrm{CO}} \\ P_w^{\mathrm{WR}}\left(a_3 v_{w,t}^3 + a_2 v_{w,t}^2 + a_1 v_{w,t} + a_0\right) & v_w^{\mathrm{CI}} < v_{w,t} < v_w^{\mathrm{R}} \\ P_w^{\mathrm{WR}}, & v_w^{\mathrm{R}} < v_{w,t} < v_w^{\mathrm{CO}} \end{cases} \tag{C1}$$

where $P_{w,t}^{\mathrm{W}}$ is the power output of the wind turbine w; P_w^{WR} is the rated power output of the wind turbine w; $v_{w,t}$ is the wind speed of the wind turbine w; v_w^{CI}, v_w^{CO}, and v_w^{CR} are the cut-in, cut-out, and rated wind speed of the wind turbine w, respectively; a_3, a_2, a_1, and a_0 are the fitting coefficients.

Step 3: Photovoltaic power output is calculated by the solar irradiance-power conversion function:

$$P^{S}_{s,t} = \eta_s S_s I_{s,t} \tag{C2}$$

where $P^{S}_{s,t}$ is the power output of the photovoltaic array s; η_s is the photoelectric transformation efficiency of the photovoltaic array s; S_s is the surface area of the photovoltaic array s; $I_{s,t}$ is the solar irradiance.

Appendix D

This appendix provides the illustrations and steps of the scenario reduction method. Note that scenarios of renewable power output generated by the Monte Carlo method are very huge, which brings an expensive computational burden for solving the stochastic optimization model. Thus, it is essential to obtain a subset of renewable power output scenarios with a limited number of scenarios and without losing the generality of the original set. The scenario reduction method is such an effective method that can reduce the scenario number and maximally retain the fitting accuracy of samples.

Assume that the number of renewable power output scenarios generated by the Monte Carlo method is N, with $1/N$ probability of each scenario (i.e., $p_s = 1/N$). The steps of the scenario reduction method are detailed as follows:

Step 1: Set an objective number of scenarios n, and specify the initial number of reduced scenarios $n* = N$.

Step 2: Calculate the Kantorovich distance D between each pair of scenarios (s_i, s_j), where D is the absolute value of power output difference between scenarios s_i and s_j, i.e., $D(s_i, s_j) = \left|P^{RES}_{i,t} - P^{RES}_{j,t}\right|$.

Step 3: For each scenario s_k, select the scenario s_l with the minimum distance $D(s_k, s_l) = \min D(s_k, s_m)$, $k \neq m$, and calculate the product of distance and scenario probability as $PD(s_k, s_l) = D(s_k, s_l)p_l$.

Step 4: Select and delete the scenario o with minimum $PD(s_o, s_l) = \min PD(s_k, s_l)$. Update the number of reduced scenarios as $n* = n* - 1$ and the probability of scenario l as $p_l = p_l + p_o$.

Step 5: If $n* = n$, present reduced scenarios and their probabilities; otherwise, reorder scenarios and return to Step 2.